

APPENDIX B

EXPLORATION ON ADAK ISLAND, ALASKA

by

David L. Butler and George V. Keller

Appendix B accompanies a report entitled "Geothermal Energy in the Pacific Region" by L. T. Grose and G. V. Keller, May, 1975. This project has been supported by the Office of Naval Research Contract Number N00014-71-A-0430-0004.

APPENDIX B - EXPLORATION ON ADAK ISLAND, ALASKA

David L. Butler and George V. Keller

Introduction

As pointed out in the body of this report, the Aleutian Islands comprise an area of active to recently active volcanism which should be favorable for the occurrence of geothermal energy. Adak Naval Base is an excellent candidate for the use of geothermal energy, inasmuch as Adak Island is located toward the western end of the active portion of the Aleutian Islands. Because of this, some exploration was carried out on Adak Island in an attempt to evaluate the geothermal potential. Seismicity and resistivity surveys were carried out on Mount Adagdak, on northern Adak, near the Naval Base (see Figure 1).

The area of interest, the northern mountainous part of Adak, is the remnants of three historically inactive[?] volcanoes. From east to west, the volcanoes are Mount Adagdak, Andrew Bay Volcano, and Mount Moffet. Although no extensive faulting has been mapped in this area, some evidence of faulting is present on the north slope[?] of Mount Adagdak. The lithology of this area includes volcanic and intrusive rocks of Paleozoic age, Tertiary to Quaternary volcanic rocks and Quaternary alluvium. The alluvium unit consists largely of glacial drift and other unconsolidated materials, including volcanic ash.

Seismicity Surveys

More than 1000 km² near Adak Island was surveyed from Oct. 22 to November 1, 1974, for microearthquakes to aid in the evaluation of the geothermal potential of the area. The survey was carried

INDEX MAP

+ 177°E
+ 52°N

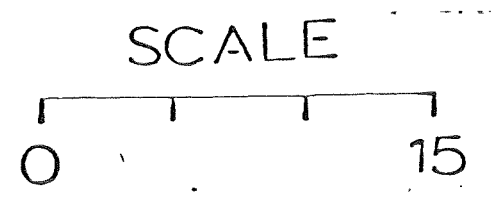
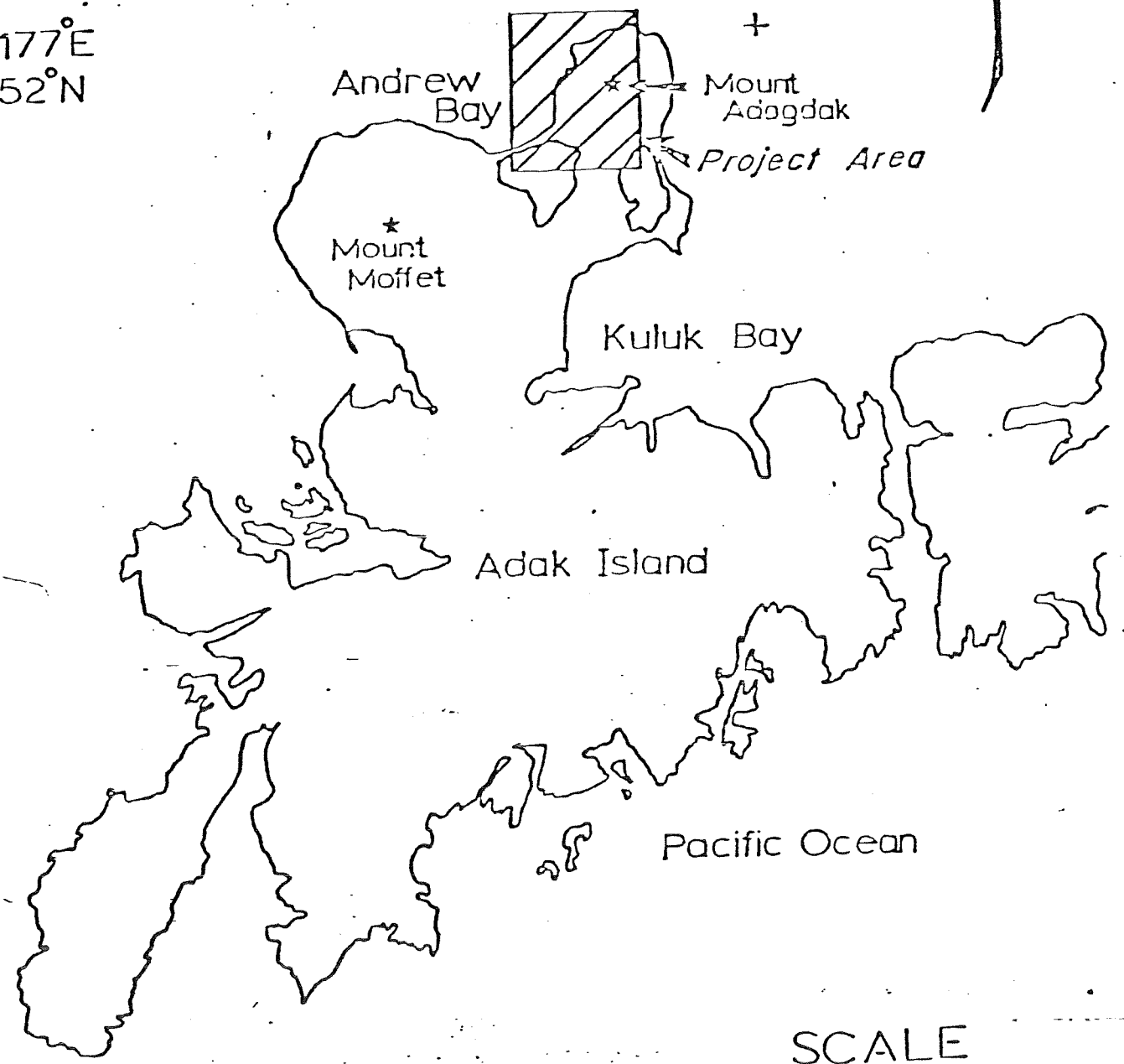


fig 1

+ 176° 30'E
+ 51° 30'N

+

of Mines. The size of the 1000 km² area is based on a detection threshold of magnitude 0 or less with at least one station recording an event within the area. The objective was to detect and locate microearthquakes and thereby map tectonically active structures.

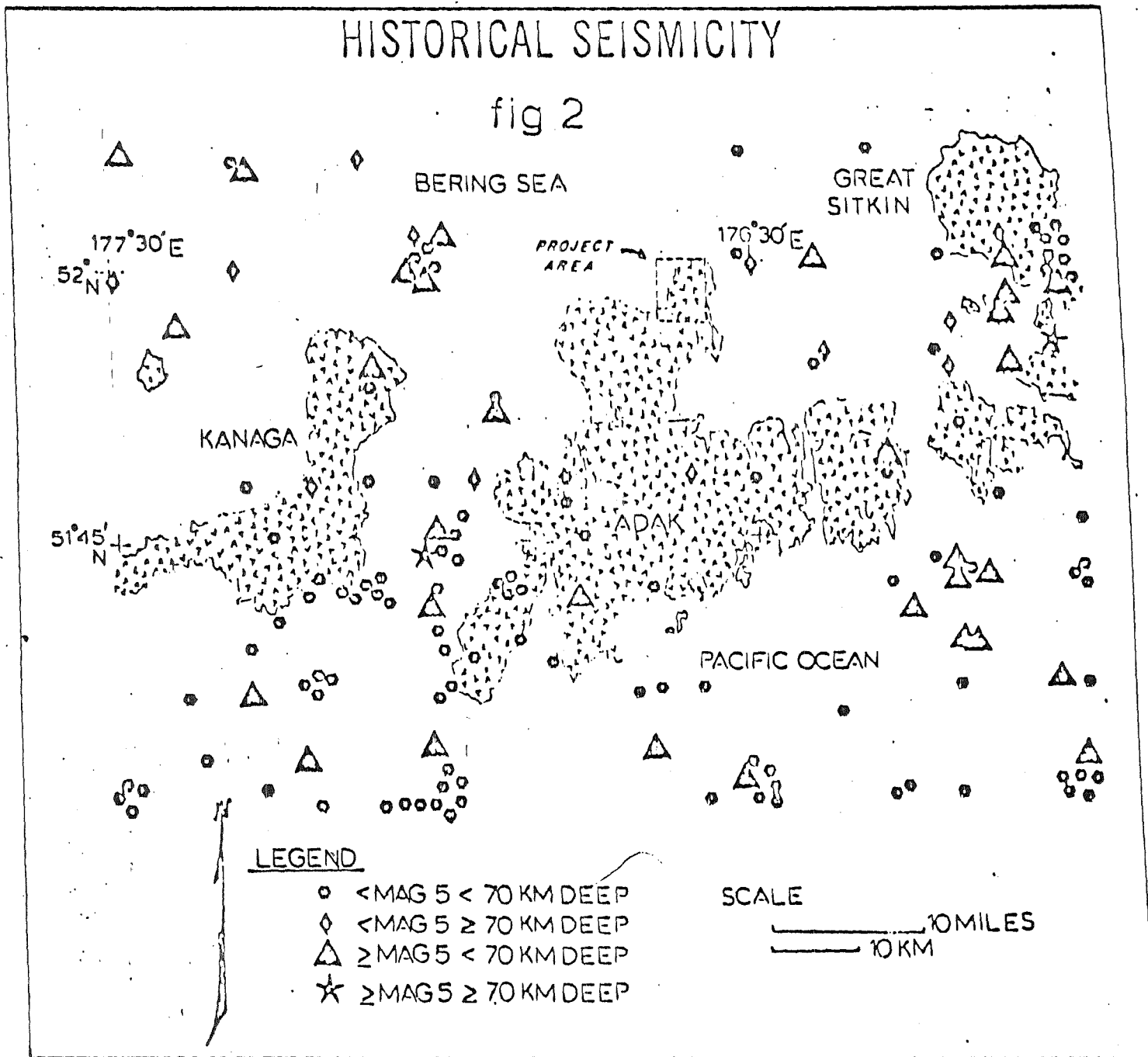
Figure 2 is an historical seismicity map of the area around the Adak Island. The Aleutian Arc is an active seismic province, however, a large number of the events shown on Figure 2 occur on or near the subduction or Benioff Zone of the Aleutian Island arc-trench system. The subduction zone is the postulated tectonic feature occurring where one crustal plate is being forced under another. In the Aleutian Islands, the North Pacific Plate is being moved in a northwesterly direction under the American Plate.

The subduction zone strikes east-west south of Adak and dips to the north to a depth of 100 to 150km beneath the island. The seismic activity associated with the subduction zone occurs at too great a depth to be of interest in this survey but the tectonic activity at depth is a manifestation of the regional stress. This same stress pattern may influence surface faulting and the shallow microseismicity of interest in this survey.

The specific project area contains no historical epicenters although several epicenters are northeast of the area of interest. In early March, 1974, 13 small earthquakes were detected by the NOAA Seismological Observatory on Adak and located near Andrew Bay and Mount Adagdak (Mr. D. Glover, personnel communication, 1974). These events are of small magnitude ($m < 3$) and are not plotted on the historical seismicity map (Figure 2).

HISTORICAL SEISMICITY

fig 2

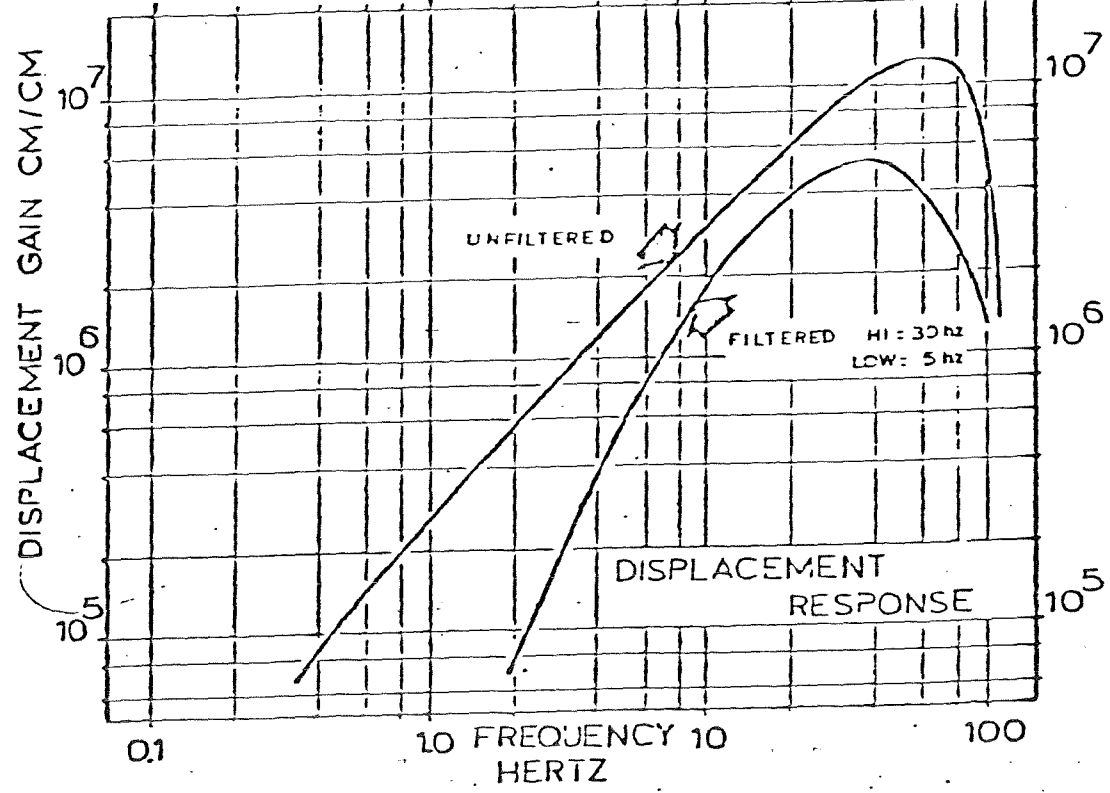
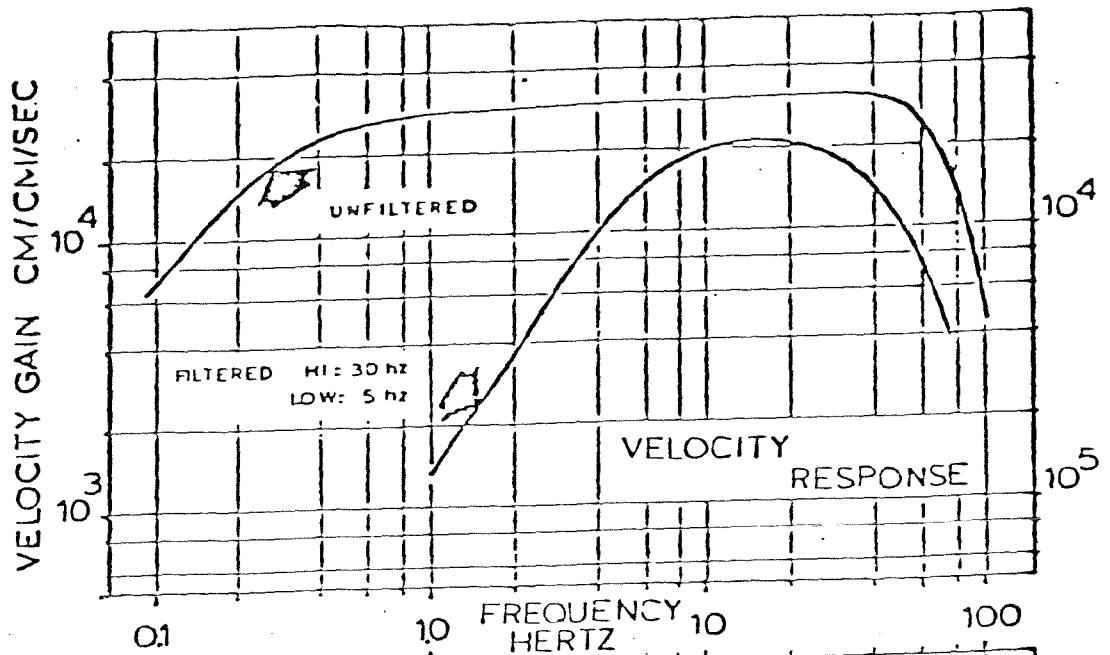


During the course of this survey, assistance and data were supplied by Mr. D. Glover, observatory director of the National Oceanic and Atmospheric Administration (NOAA), Seismological Observatory, Adak, Alaska. The data supplied includes arrival times, S-P times and magnitudes of several local earthquakes. His enthusiastic assistance is gratefully acknowledged.

The next section of this paper outlines the instrumentation and operational methods employed in the field work. The observations and analysis are given in a section and are followed by an interpretation of the results. Recommendations are listed in the last section of the body of the report. The appendix is a listing of times, locations and magnitudes of the local earthquakes detected during this survey.

Instrumentation and Operational Summary

Seven Sprengnether Instrument Co. MEQ-800-B portable seismic systems were used for this survey. Each system consists of a Mark Products model LC-4, 1-hz natural-frequency vertical seismometer, gain-stable amplifier, integral timing system, and smoked paper recording with 0.025mm stylus width and 120mm/min recording speed. The frequency characteristics of the instrument are summarized in Figure 3 (note that both the velocity response and the displacement response are plotted; displacement response at a particular frequency, f , is obtained by multiplying the velocity response by $2\pi f$). Gain changes are by 6db steps from the typical operating level of +96db plotted in the figure.



INSTRUMENT RESPONSE

fig 3

INSTRUMENT RESPONSE IS PLOTTED FOR 96db GAIN

Clocks were synchronized daily with a master clock, which was synchronized with WWV. Clock drifts between synchronizations were below expected record reading errors, therefore no corrections were necessary. Records were read to ± 0.03 sec for P arrivals and ± 0.10 sec for S-P times. Amplitudes, peak to peak, were read to the nearest millimeter, and durations to the nearest 0.5 sec.

Despite the poor working conditions, considerable effort was made to locate stations on hardrock outcrops (crystalline exposures or well compacted sediments). All stations were operated at the gain limit allowed by ambient background noise. Station locations of the array operated for ten days are illustrated in Figure 4 and listed in Table 1. Stations 1 through 9 were operated by MicroGeophysics Corporation; z1-z5 and AD8 by NOAA. Details of the operation of stations 1 through 9 are shown in Table 2. The NOAA stations, which are operated continuously, are part of the permanent tsunami-warning network of NOAA. The operation schedule (Table 2) shows the gains and the time periods of individual station occupations.

MAP OF STATION LOCATIONS

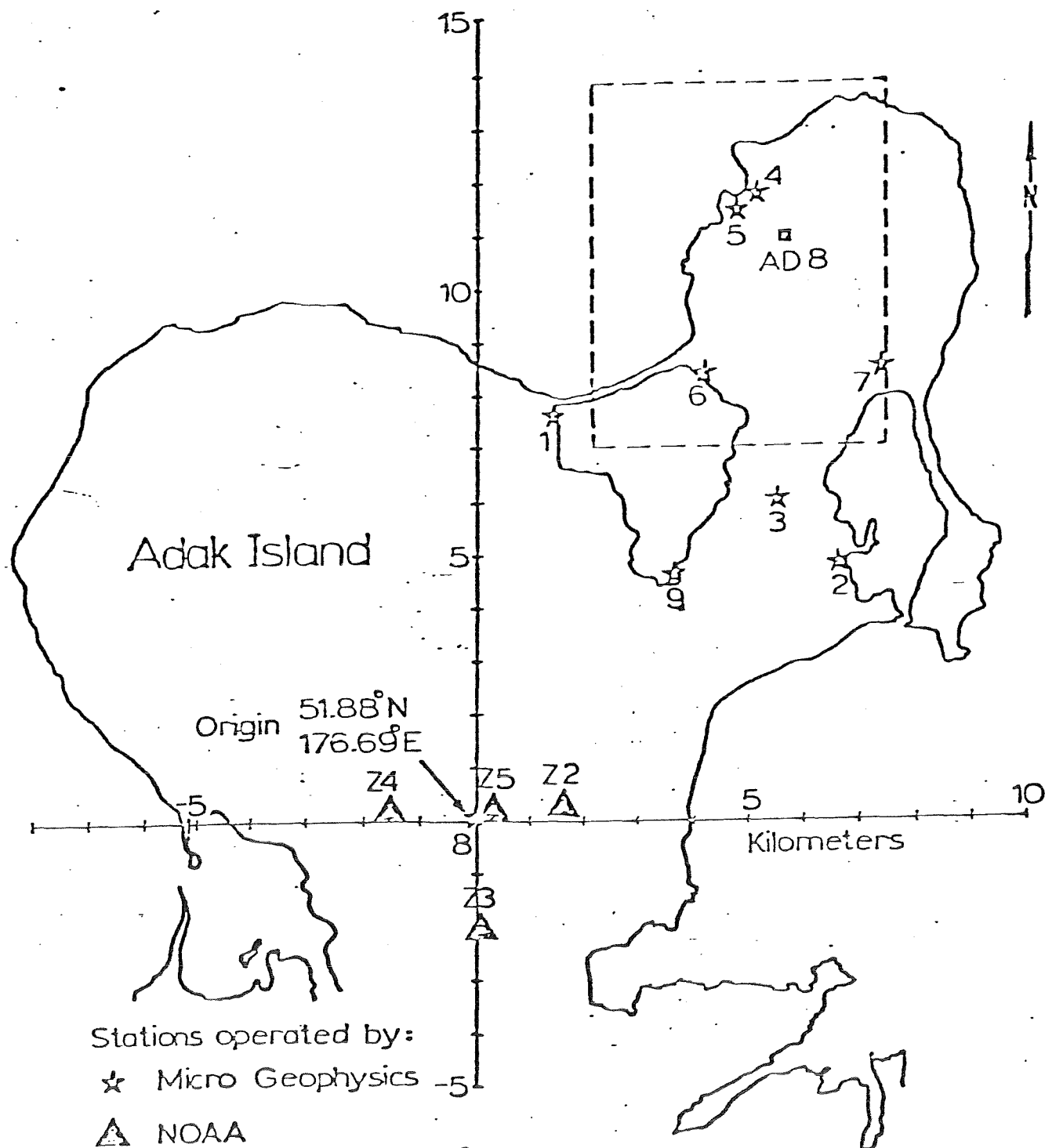


fig4

STATION COORDINATES

TABLE 1

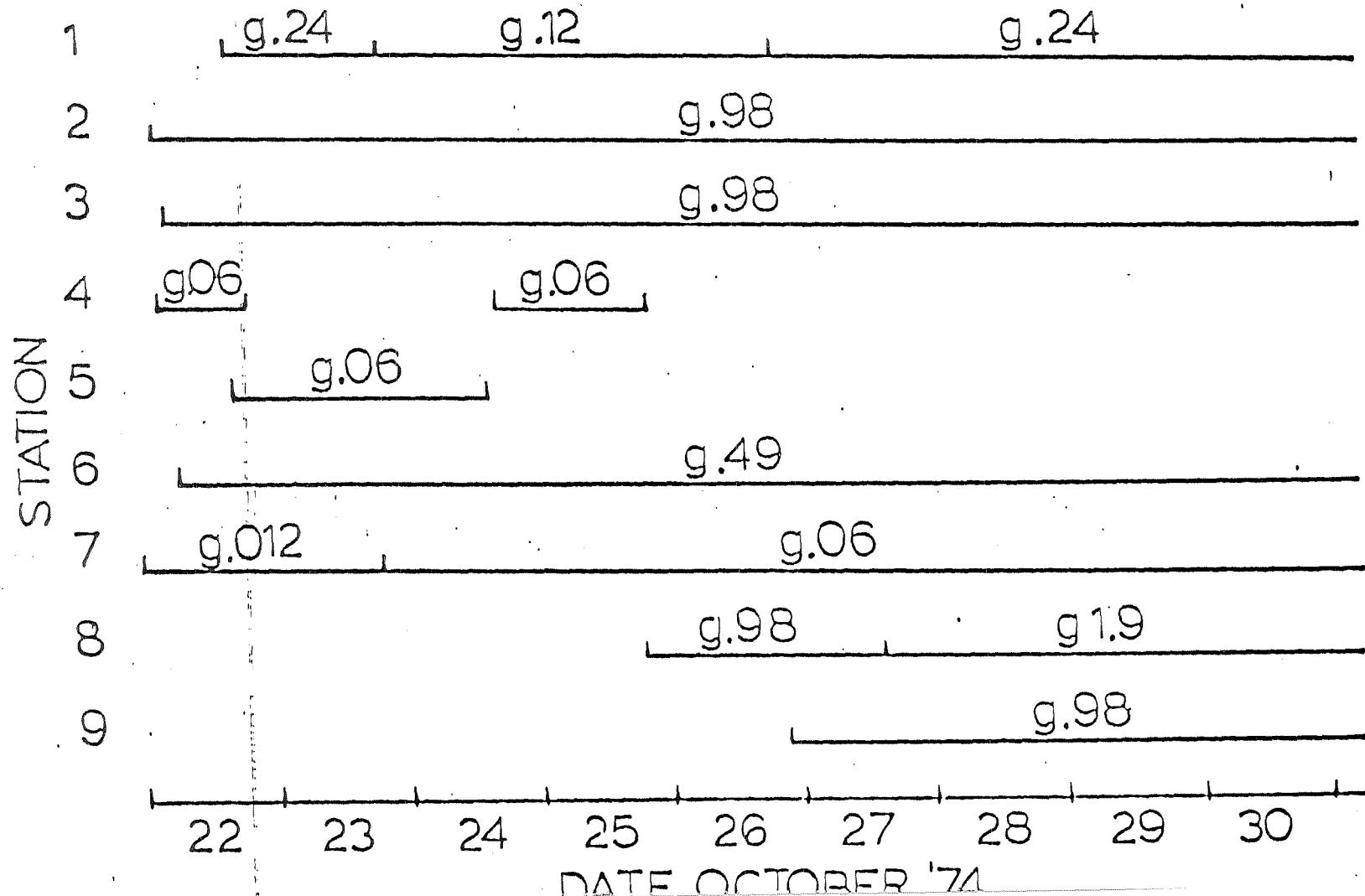
<u>Station</u>	<u>X* in km</u>	<u>Y* in km</u>	<u>Z* in km</u>
1	1.33	7.60	0.00
2	6.62	4.95	0.00
3	5.38	6.03	0.03
4	5.15	11.75	0.09
5	4.80	11.40	0.09
6	4.15	8.42	0.03
7	7.31	8.58	0.05
8*	0.00	0.00	0.09
9	3.70	4.60	0.03
z2	1.70	0.35	0.06
z3	0.05	-1.90	0.03
z4	-1.60	0.15	0.09
z5	0.15	0.05	0.09
AD8	5.60	11.00	0.24

* The origin is located at station 8 (latitude 51.88°N, longitude 176.69°W). Positive X and Y are east and north respectively.
 Z is the station height above sea level (altitude).

OPERATION SCHEDULE

table 2

g.12 = gain/one million at 20 Hertz
filters at 5-30 Hz



Observations and Analysis

Events were regarded as seismic in origin if they appeared on two or more stations with time differences corresponding to seismic velocities or if they were similar in appearance to other larger events which were well recorded. Seismic events were considered local if they had S-P times of less than four seconds.

The S-P time is a characteristic indicator of distance to the epicenter of an event. The S-P time is the difference between the arrival time of the S or shear wave and the P or compressional wave. The two body waves propagate by different mechanisms and at different velocities dependent on the parameters of the transporting medium. The S-P time is thus a function of the distance traveled.

An example of a local event near Adak is shown in Figure 5. Regional and teleseismic (distant) events with S-P times greater than four seconds, were considered outside the scope of this survey and therefore no attempt was made to locate them. The four-second S-P time cut-off for local events is an arbitrary limit chosen by the interpreter.

Local events timed on four or more stations were located using a generalized inverse computer program. This program assumes a velocity model and least-squares fits calculated travel times to the observed arrival times. The velocity structure in the project area can be estimated from a layered crustal velocity model of the Adak region developed by the USGS (Engdahl, 1974). Figure 6 illustrates the USGS model and two

EXAMPLE OF A LOCAL EVENT

GAIN X
1000

STATION
NUMBER

560

2

560

3

560

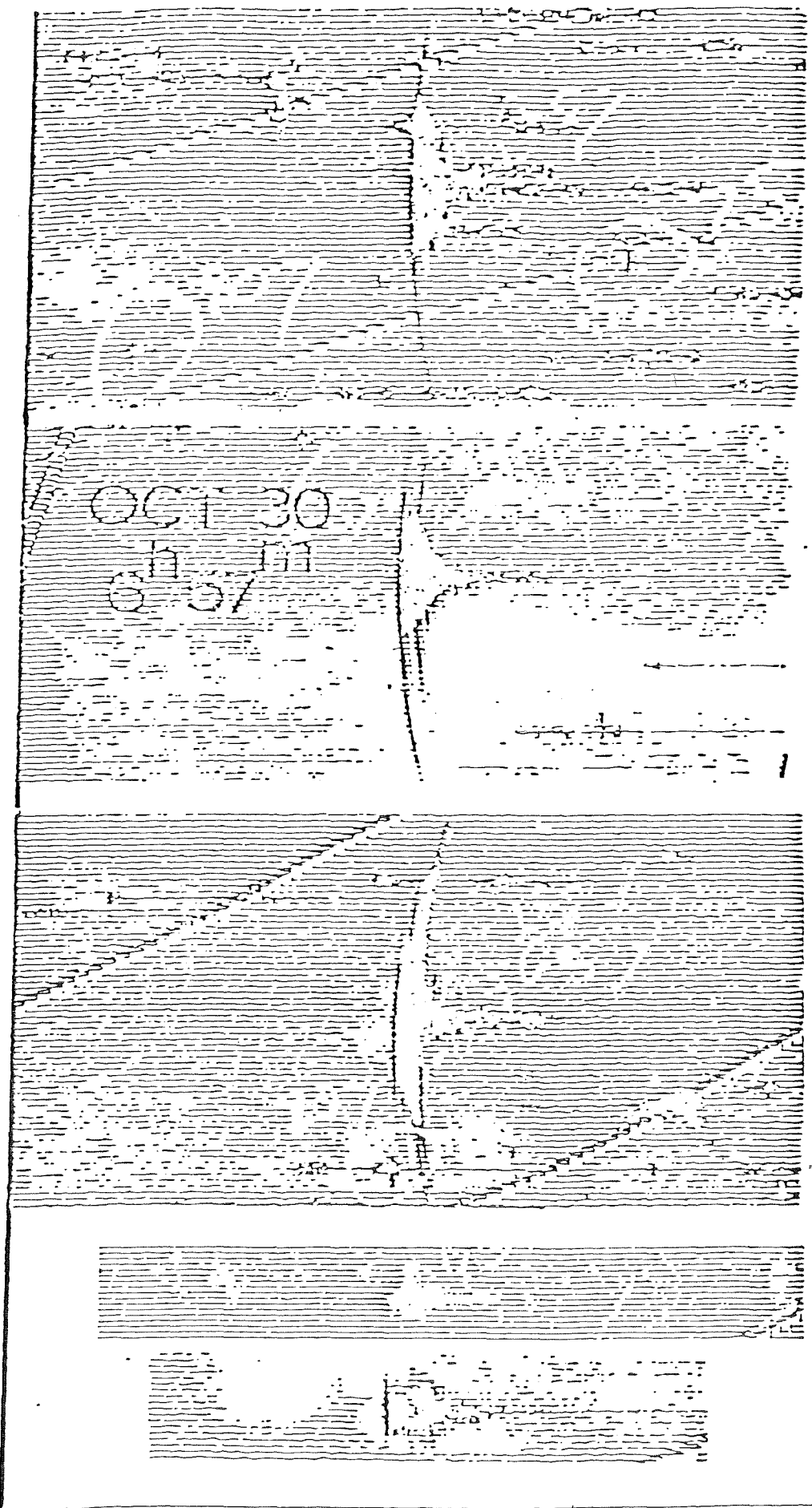
9

35

7

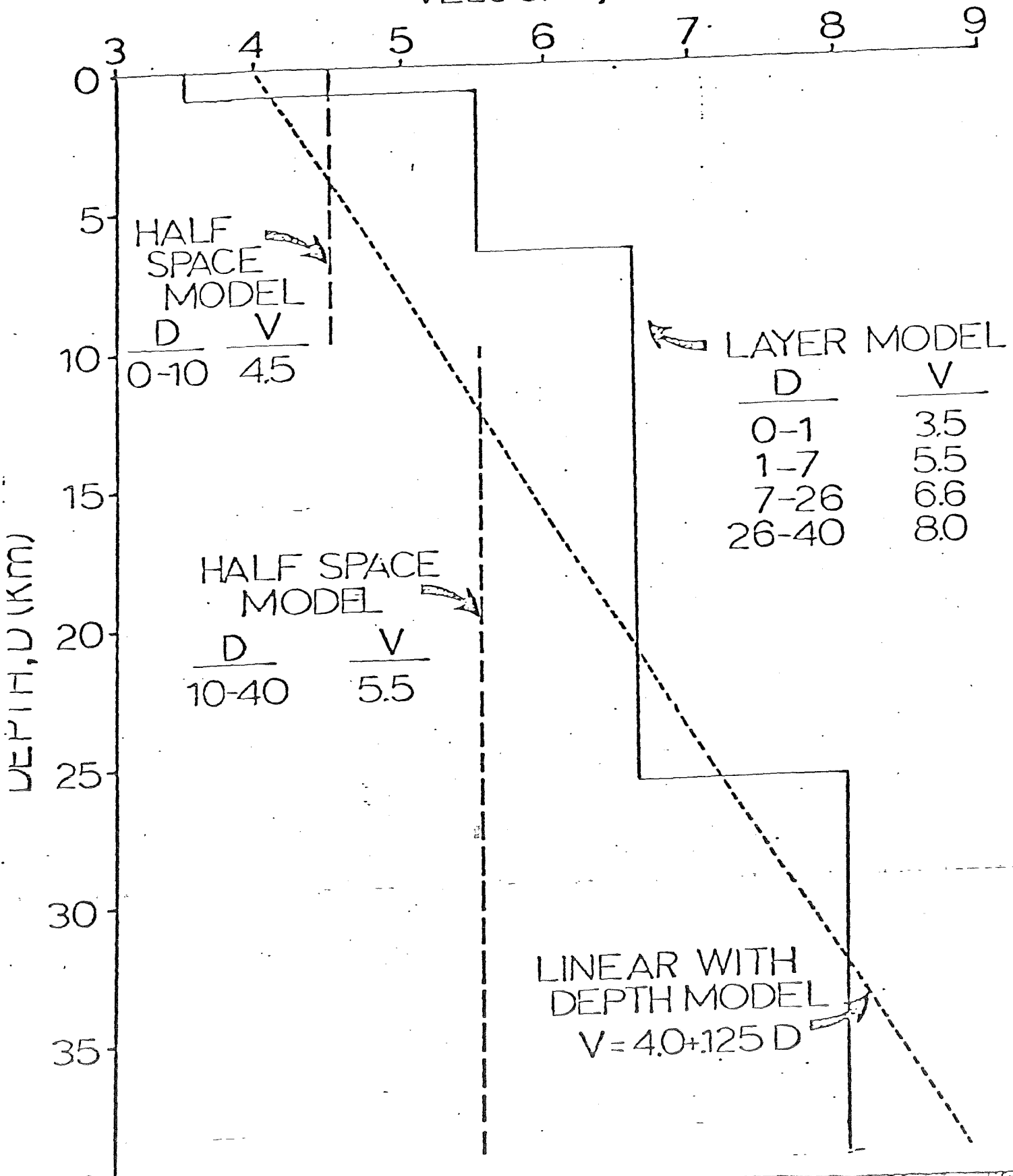
1130

8



OCT 30
11 37 AM

VELOCITY, V (Km/sec)



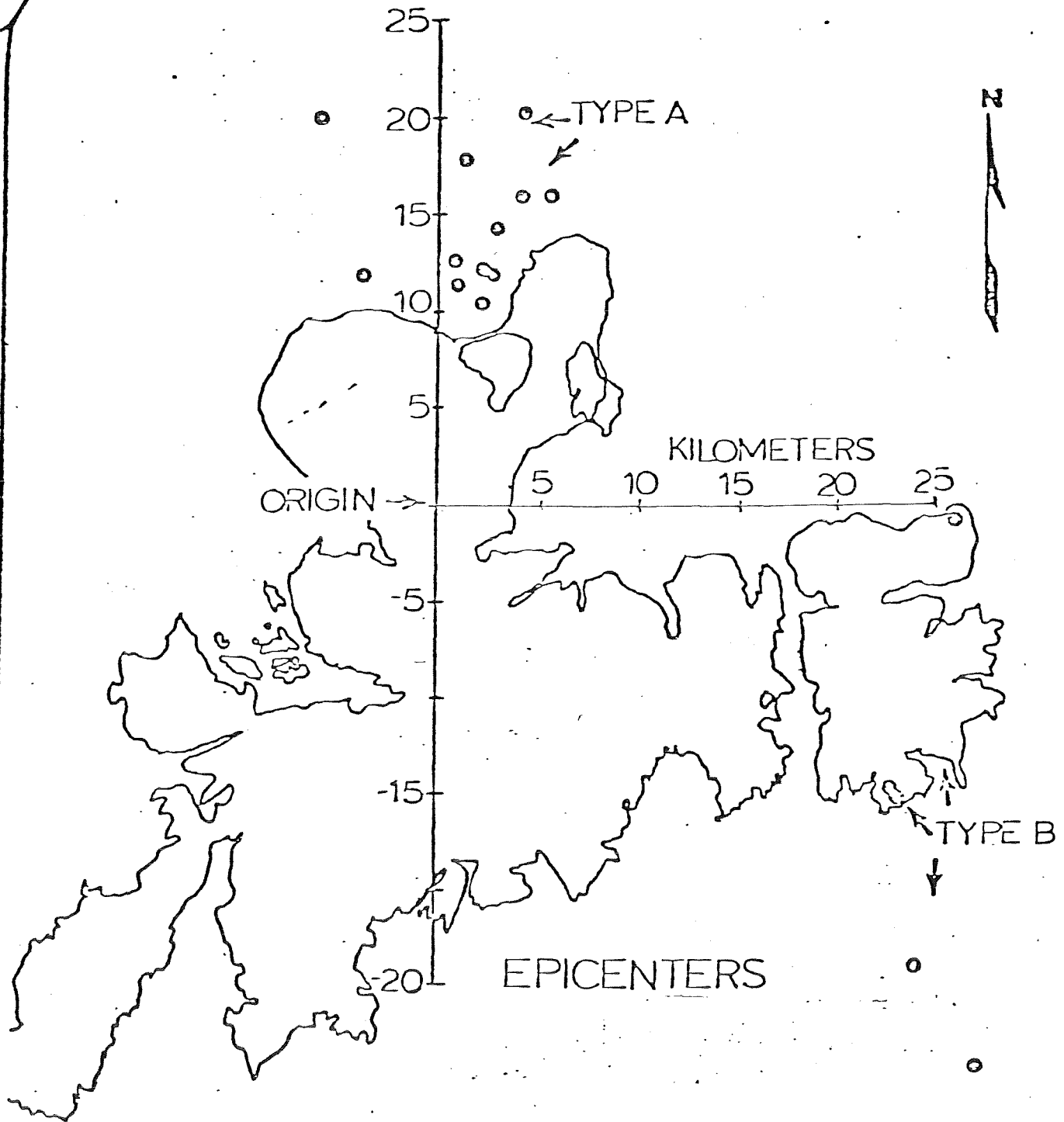
other velocity structures, a half-space model and a linear velocity-increase-with-depth model. The half-space model was used to test the picked arrival times and the sensitivity of the locations to velocity changes. The constant velocity model obtained good fits with no anomalous station residuals. The velocities obtained with the half-space model agree with the averaged velocities of the layered model. The model that produced the best fits and lowest residuals in the project area was the linear velocity-increase-with-depth model. This model is in general agreement with the layered model and it produced station residuals on the order of the picking error (± 0.03 sec).

Figure 7 shows all located events and illustrates that the local seismicity is confined to two areas. Events from these two areas were identified by using S-P times and signature similarities and were classified as "type A" or "type B" events. Figure 8 shows a plot of the cumulative number of events recorded during the survey of each type. Type A events were recorded at a rate of four events per day, type B events at a rate of three per day when there was activity.

Type B events were located 30 to 40km southeast of Adak. Due to the distance from the array, the epicenter location precision is about ± 4 km. Because these events are well outside the area of interest, no further analysis was performed.

Twenty six events denoted as type A were located in the project area. The precision of location for these events is about ± 1 km in plan and ± 2 km in depth. The events occur within

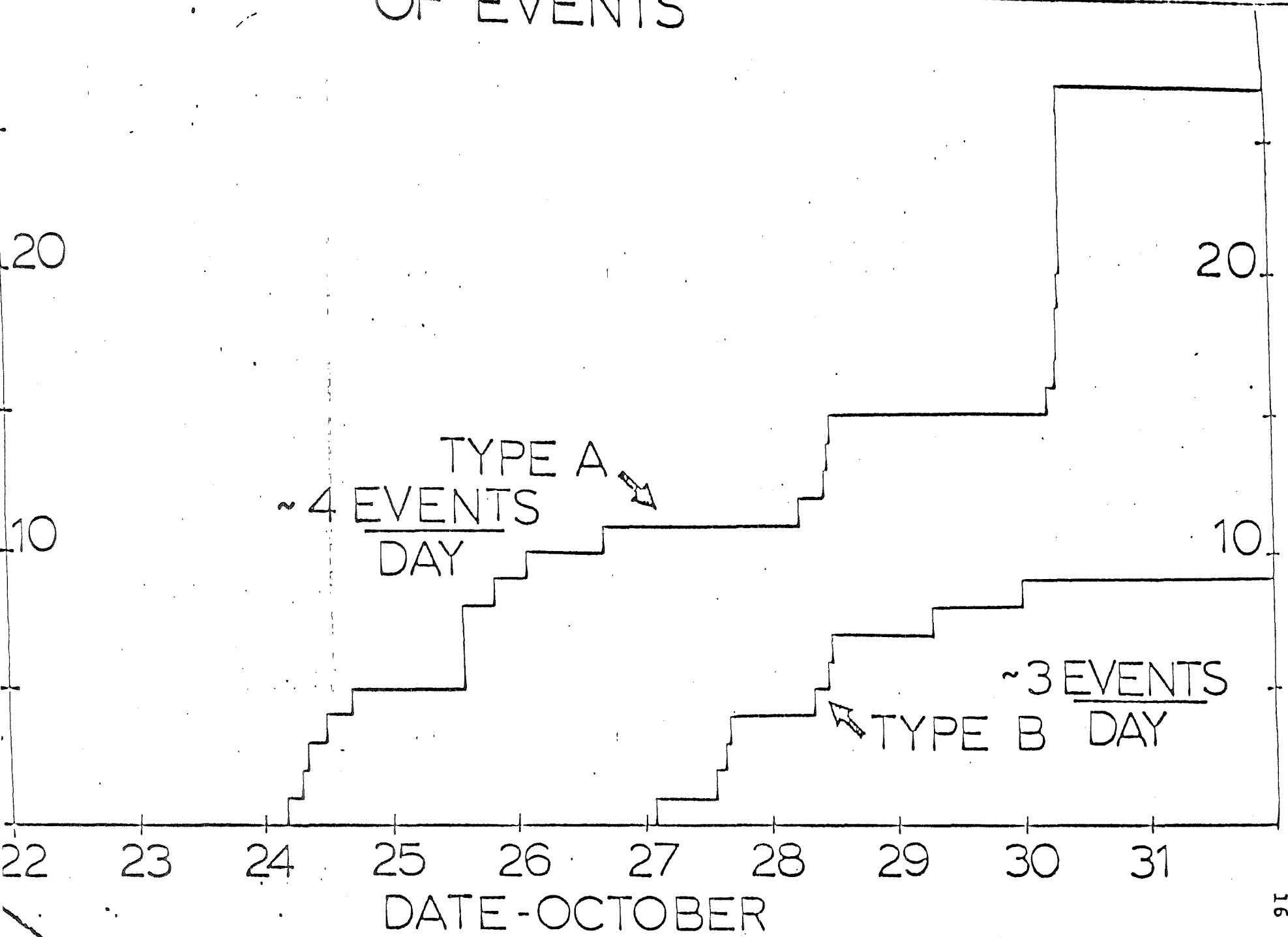
LOCATED EVENTS



THIS MAP SHOWS ALL LOCATED EVENTS AND ILLUSTRATES THAT THE LOCAL SEISMICITY IS CONFINED TO TWO AREAS

fig 7

OF EVENTS



DATE-OCTOBER

fig 8

LOCATED TYPE A EVENTS

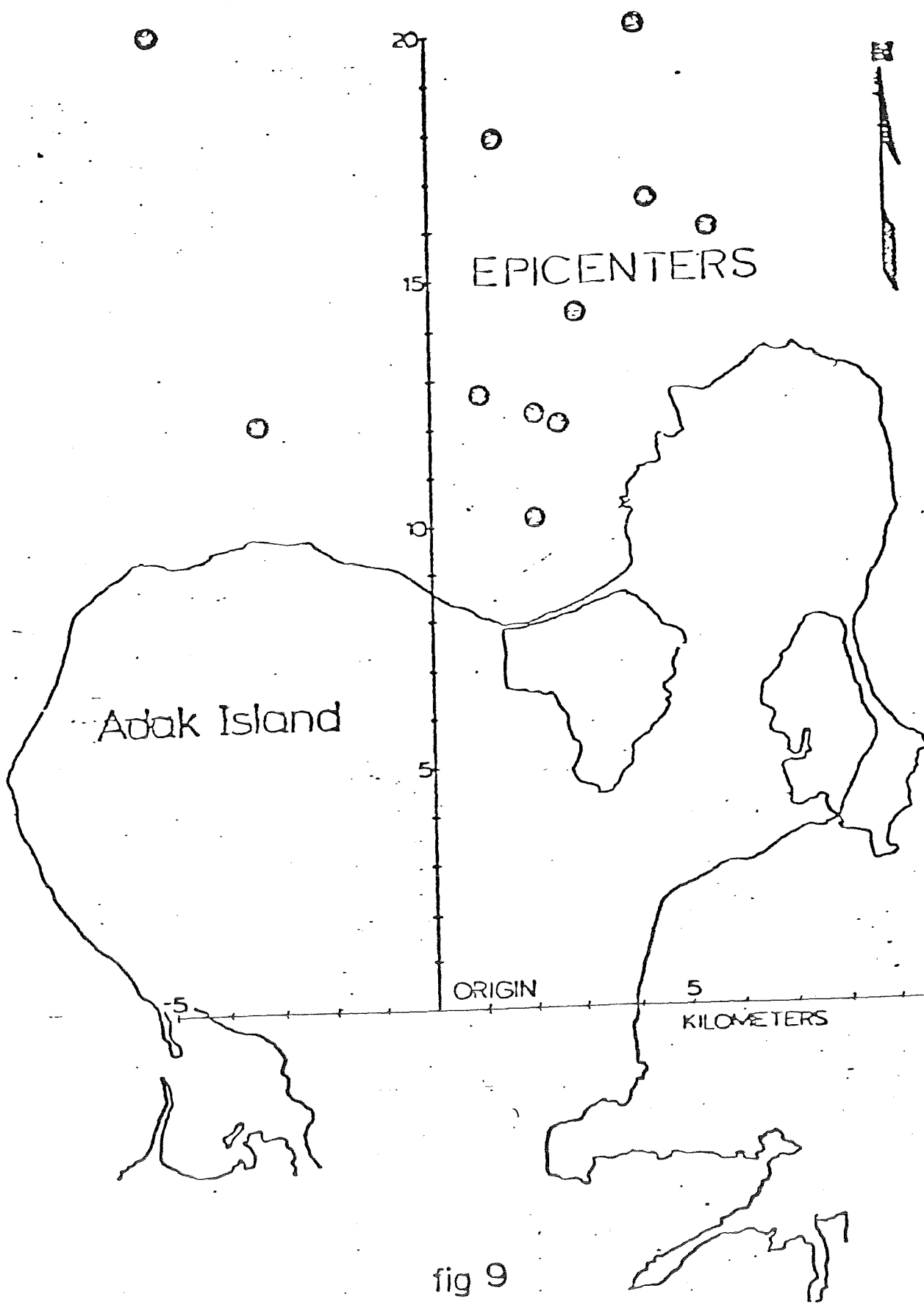


fig 9

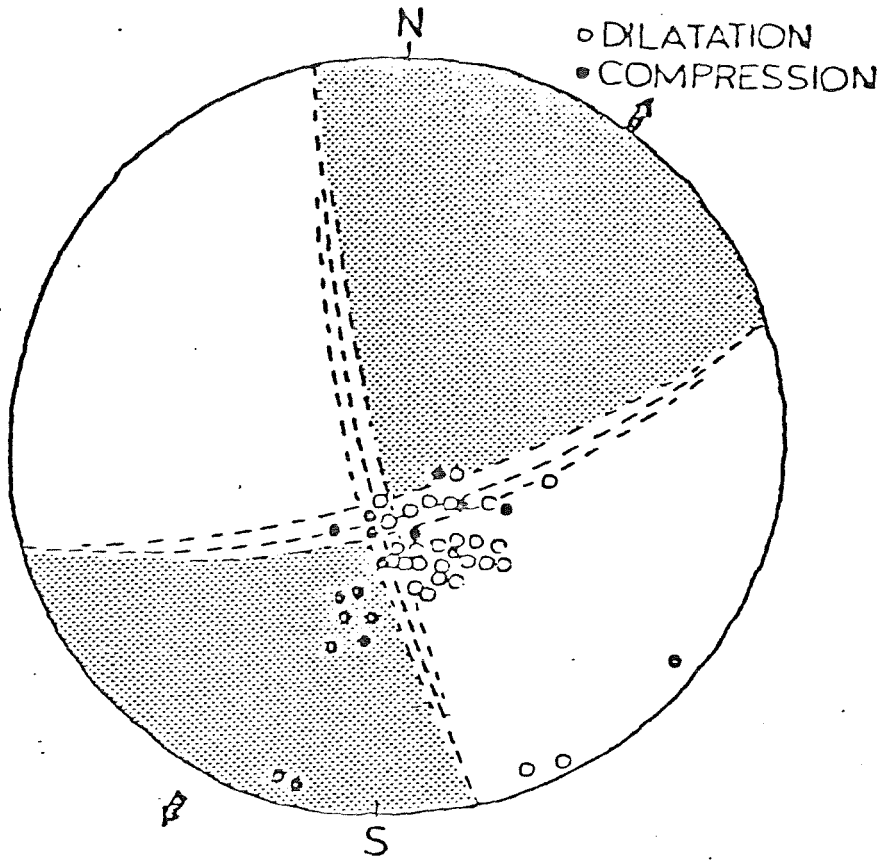
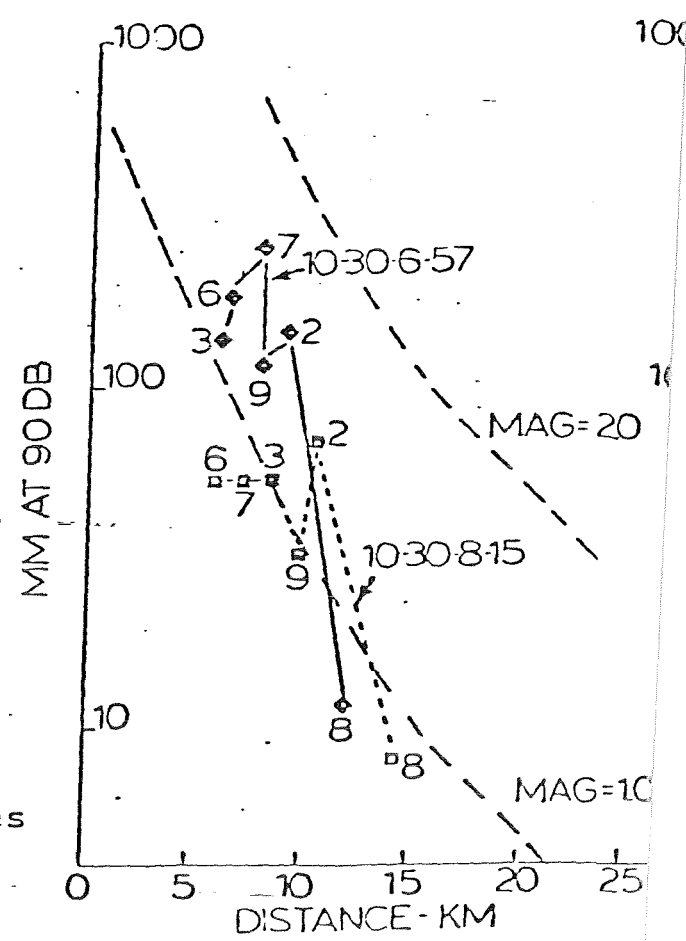


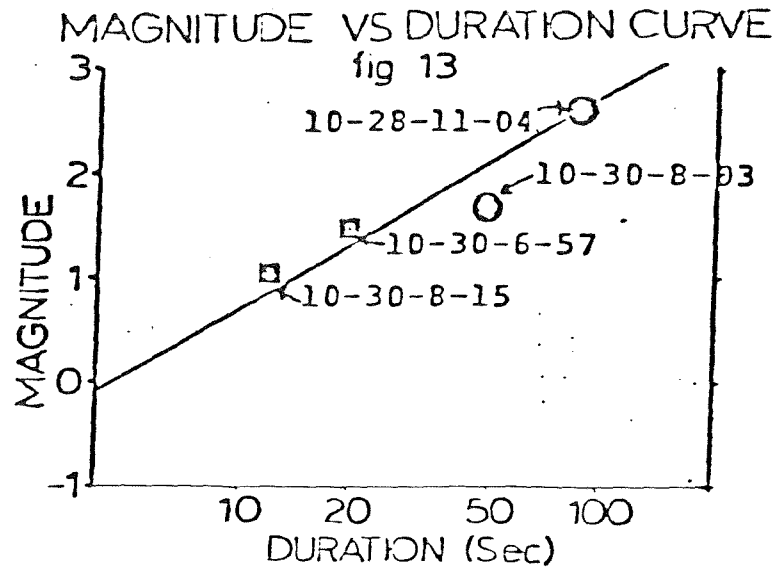
fig 11

solutions from the two methods agree well within reasonable limits of accuracy.

To estimate the level of seismicity some attention must be paid to the size or magnitude of an earthquake. In this survey an amplitude versus distance plot (see Figure 12) was constructed for two local events (October 30 at 6^h57^m and at 8^h15^m). The magnitude of these events was determined by using curves established for microearthquakes

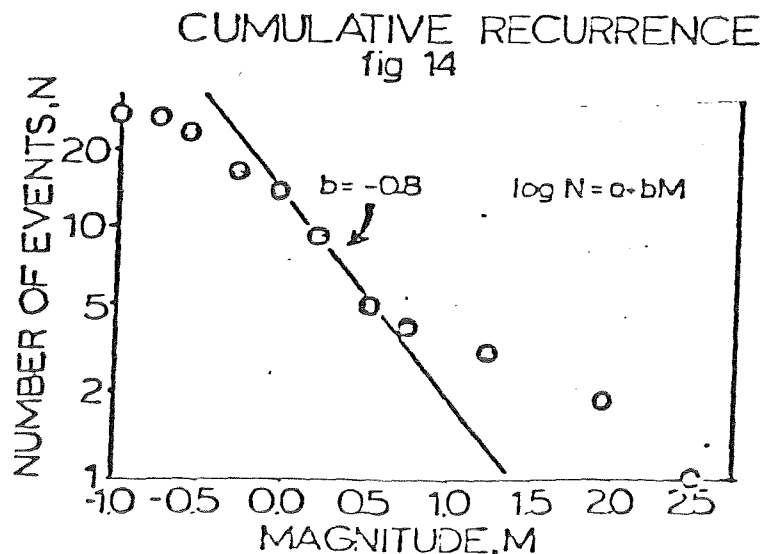
AMPLITUDE VS DISTANCE





by Brune and Allen (1967). Magnitudes from two other larger events (October 28, 11^h04^m and October 30 at 8^h03^m) were supplied by the NOAA Adak Observatory. These four events were then used to determine a magnitude versus duration curve (see Figure 13). To correct for local geologic effects all durations were measured at station 3.

From the magnitude versus duration curve, all detected events were assigned a magnitude. The resulting cumulative recurrence curve (a plot of the log of the number of events of a given magnitude versus the magnitude) is shown in Figure 14.



The slope of this linear relationship is often called the b-slope. A b-slope of -0.8 is shown with the data for reference.

Figure 15 shows the relationship between Poisson's ratio and the velocity ratio. The often assumed value of Poisson's ratio of 0.25 is shown, but an increase of up to 0.1 often occurs when a rock is fractured. The velocity ratio is defined as the ratio of the compressional wave velocity (V_p) divided by the shear wave velocity (V_s). Poisson's ratio is defined as the ratio of the transverse contraction to the longitudinal extension of a rod subjected to an axial load. Poisson's ratio is also a qualitative measure of the amount of fracturing present in a rock mass. Therefore a map indicating variations of Poisson's ratio or the velocity ratio may indicate areas or volumes with anomalous fracturing and resultant high permeability.

Figure 16 is a plot of arrival time versus S-P times for eight events recorded by this survey. This relationship, often called the Kadati diagram method, has been discussed by others (Semyenov, A.N., 1969; Nersesov, et.al., 1971; Kisslinger, Engdahl, 1973). These eight events showed good S-wave breaks and were well recorded across the net. Figure 16 gives two values for each slope. The A parameter is the slope of the linear relationship which indirectly gives the velocity ratio and σ gives the corresponding Poisson's ratio from Figure 15.

Figure 17 is a plot of the velocity ratio with time. Variations from a constant velocity ratio have been used to study premonitory phenomena for large earthquakes with some

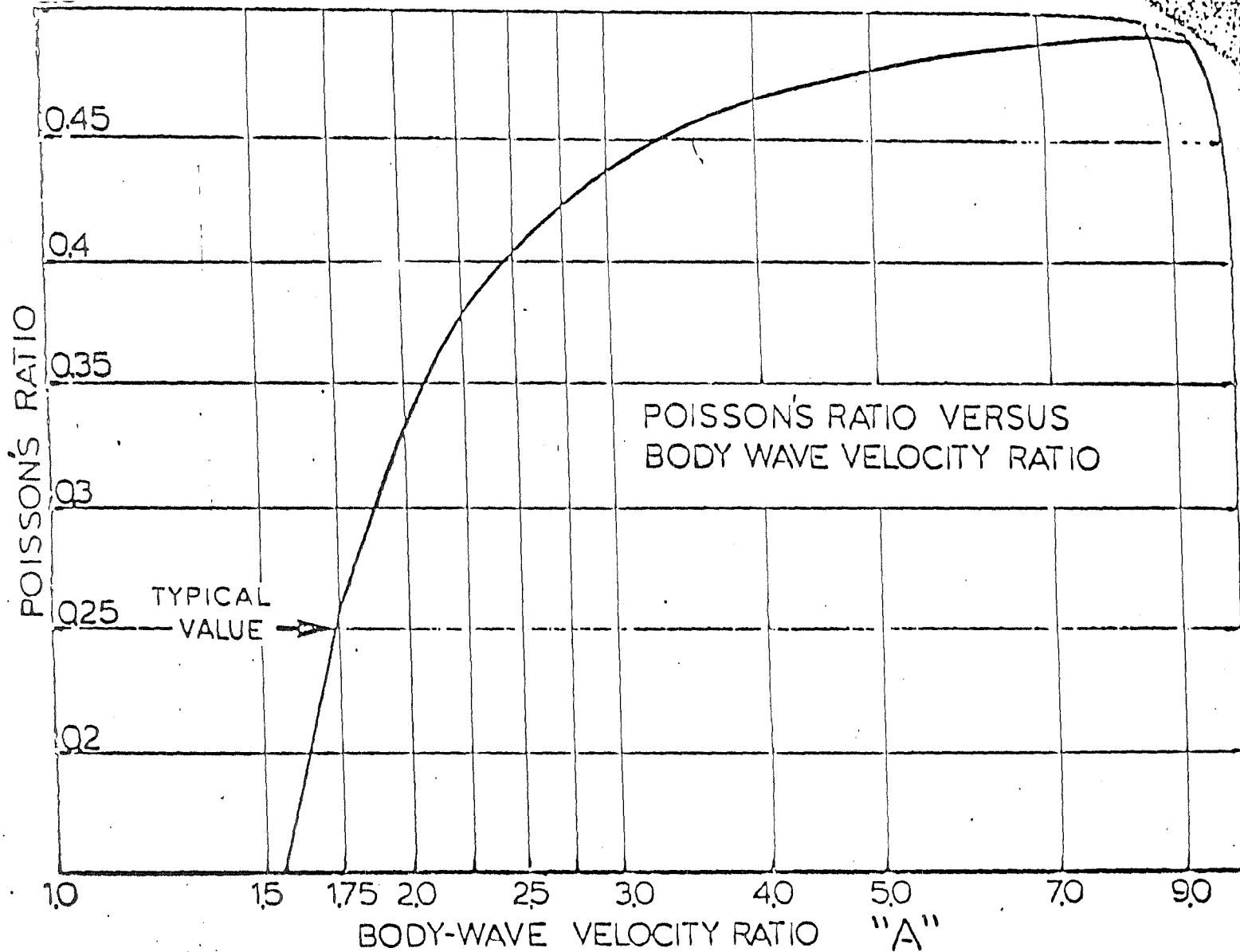


fig 15

THIS FIGURE SHOWS THE RELATIONSHIP BETWEEN POISSON'S RATIO AND VELOCITY RATIO. THE OFTEN ASSUMED VALUE OF 0.25 IS INDICATED.

WADWAI DIAGRAMS

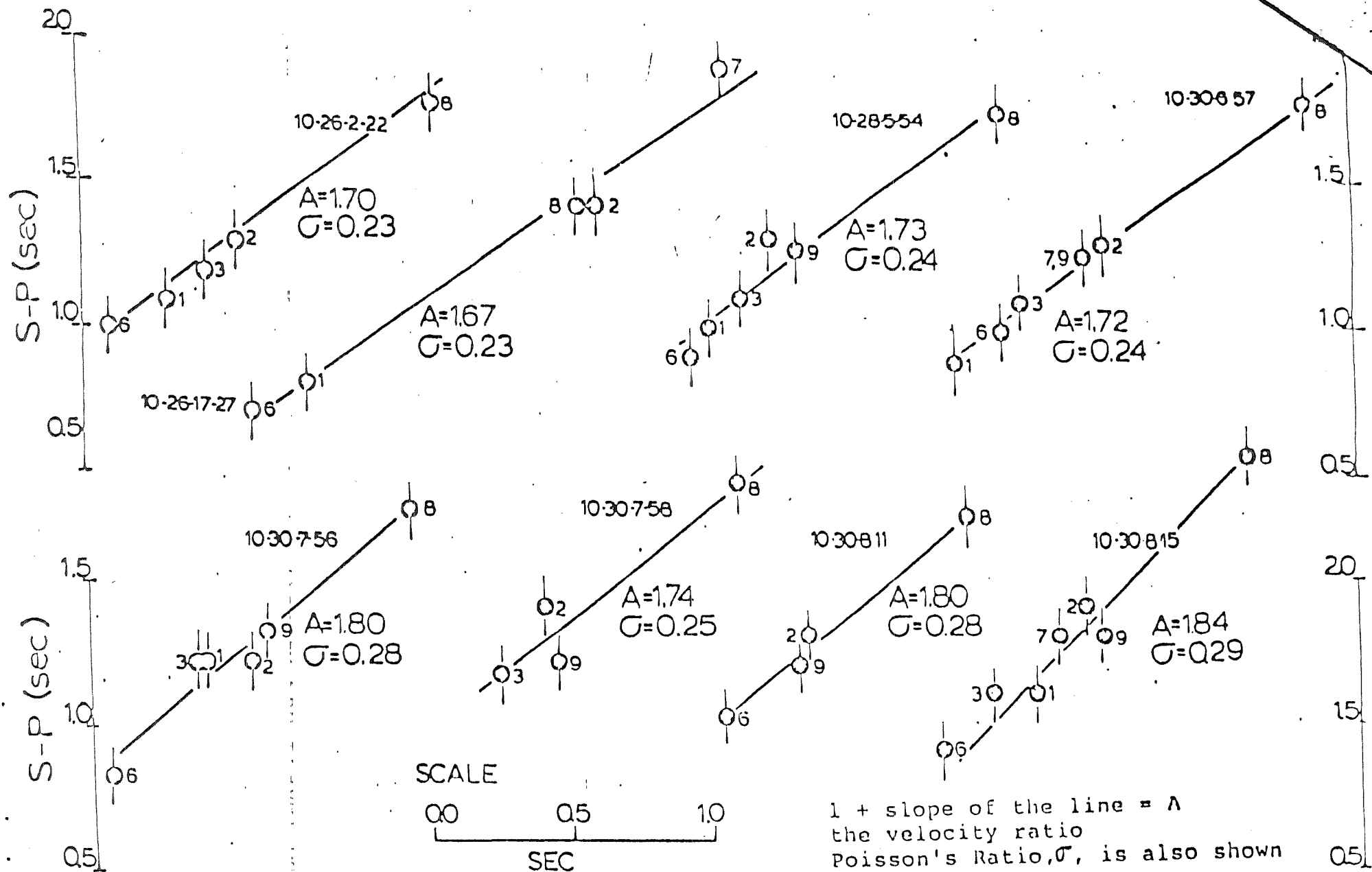
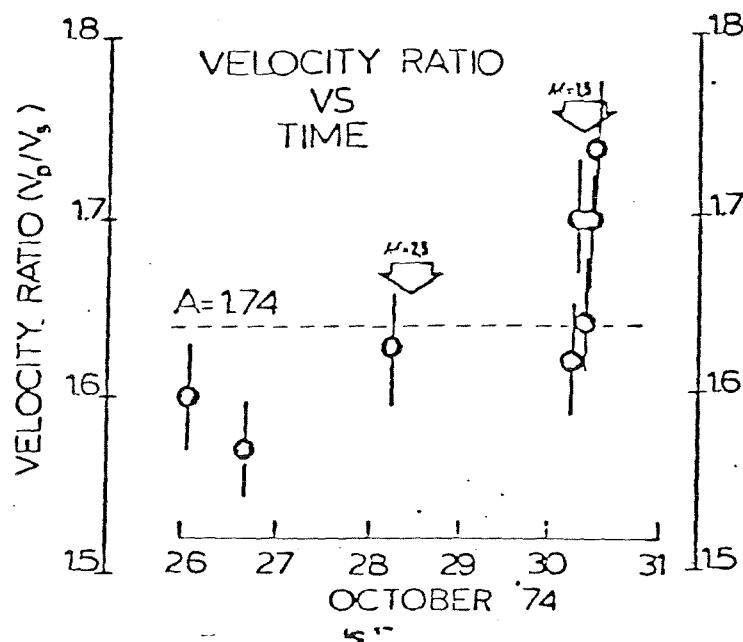


FIGURE 16

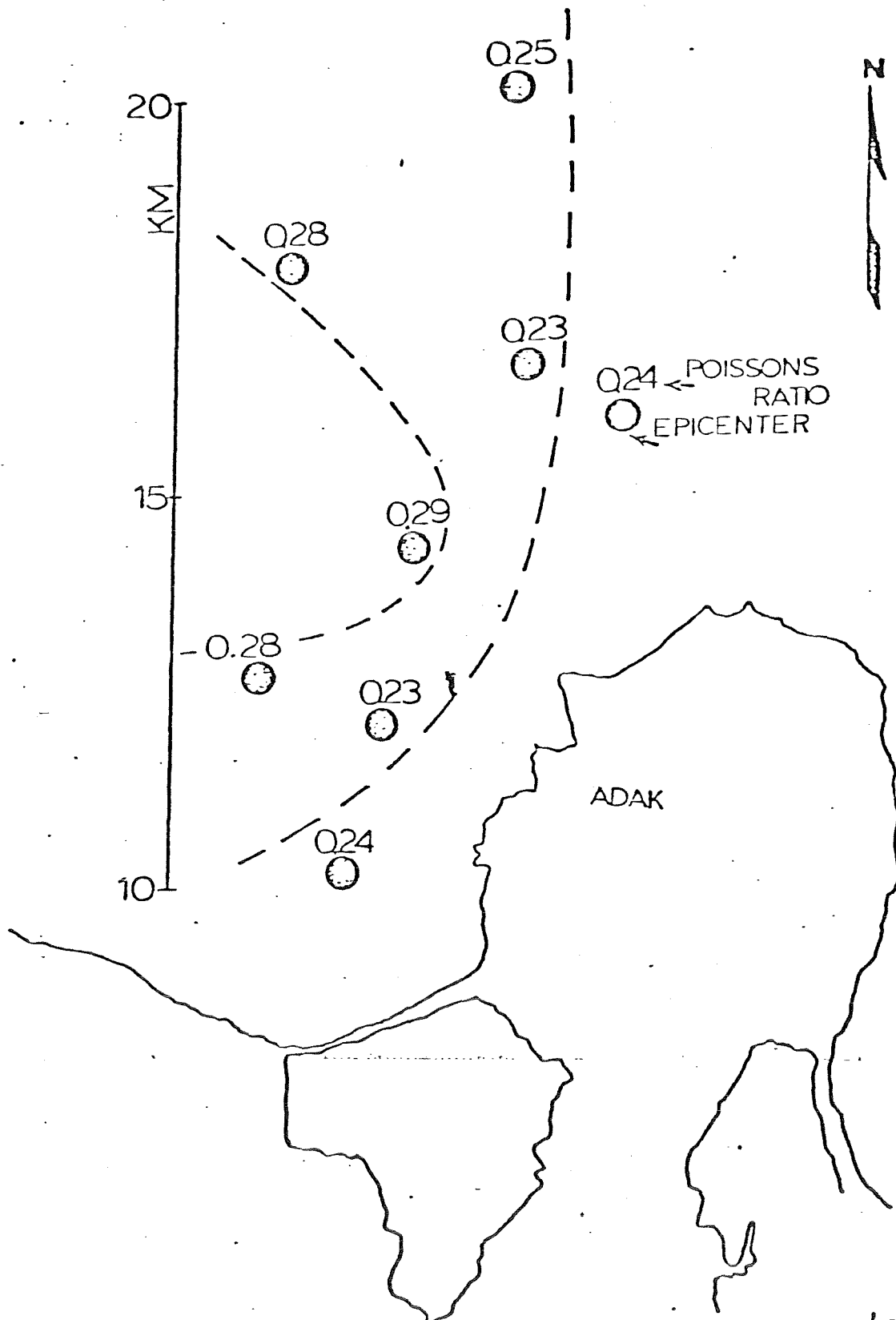
PLOT OF S-P TIME VERSUS P ARRIVAL TIME. EACH CURVE REPRESENTS A
STATION NUMBER. EACH DATA POINT (IDENTIFIED BY STATION NUMBER) REPRESENTS

success (Semyenov, 1969; Nersesov, 1971; Kisslinger, Engdahl, 1974). The short time-sampling period of this survey precludes any prediction from this data but the spatial distribution of Poisson's ratio can be interpreted.



To locate an anomalously fractured zone, a map of the observed Poisson's ratio (plotted at the epicenter) was made (see Figure 18). Note that the form lines indicate trends in the data and are not contour lines. The Poisson's ratio was assumed to be more heavily influenced by the source region and mechanism than by the travel path, therefore the value was assigned to the epicenter. Assignment of the value to the travel path would complicate the display, but the same conclusion would be derived from the alternate display. Figure 18 produces a consistent picture of Poisson's ratio increasing to the west and with depth along the fault.

POISSONS RATIO

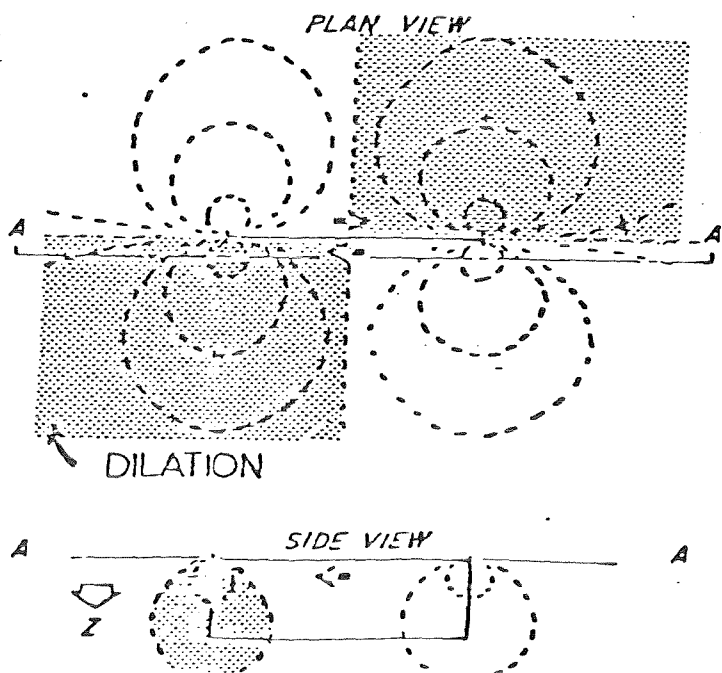


FORM LINES REPRESENTING CONSTANT POISSON'S RATIO

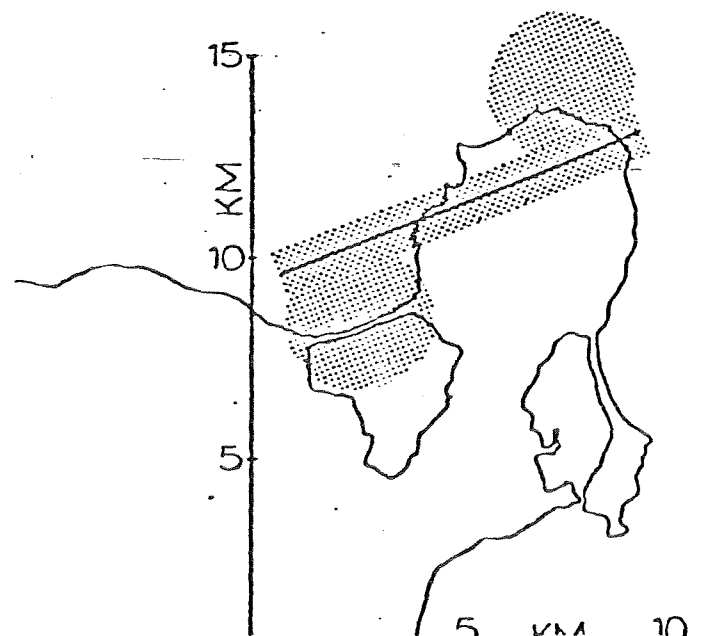
fig 18

The anomalous distribution of Poisson's ratio and its spatial relation to the geologic features can be explained by a theoretical model. This model is calculated by assuming a Volterra-type dislocation for the fault mechanism. For this model, the volume strain or dilation can be calculated around the fault given the spatial geometry of the fault plane. The Volterra-type dislocation model assumes that a homogeneous half-space is broken along a distinct plane and, after displacement, is welded back together. The half-space, which was initially stress free, now is subjected to a regional stress (manifested by the volume strain, which can be contoured) created by the dislocation at the "fault plane". The dilation or volume strain around such a dislocation model has been calculated by Yeatts (1975). Figure 19 shows a plan and cross section view of the dilation around a right-lateral, strike-slip fault dislocation.

DILATION MODEL



POTENTIAL GEOTHERMAL AREA



The shaded areas represent areas under dilatation and unshaded areas are under compression. The region of most severe volume expansion can be expected to exhibit microfractures, demonstrated by an increase in Poisson's ratio, leading to increased permeability.

Resistivity Survey

A resistivity survey was carried out in the Mount Adagdak peninsula area during the period October 25 to November 5, 1975, by a party under the supervision of Dr. Paul Donaldson of the Colorado School of Mines. The rotating dipole technique, as described by Tasci in Appendix A of this report, was used. Operations in the field on Adak in late Fall are fraught with difficulties, largely induced by the cold, wet, and windy weather. Relatively few measurements were made before the survey had to be terminated, and the resistivity survey must be considered to be only preliminary in nature.

In the rotating dipole method, field data are obtained by making measurements of electric field intensity around a pair of bipole sources located at a single site, but with different orientations. For the Adak survey, a pair of sources, each 700 meters in length, was placed on the southwest slope of Mount Adagdak, as shown on the map in Figure 21. Currents of a few amperes were used to excite these two source bipoles. This is less than normally used in dipole mapping surveys, but only a small motor generator set was available for the survey, and grounding resistances were surprisingly high.